A mechanism-based parameterisation scheme to investigate the association between transmission rate of COVID-19 and meteorological factors on plains in China

Changqing Lin [a], Alexis K.H. Lau [a,b,*], Jimmy C.H. Fung [a,c], Cui Guo [d], Jimmy W.M. Chan [a], David W. Yeung [a], Yumiao Zhang [a], Yacong Bo [d], Md Shakhaoat Hossain [a], Yiqian Zeng [d], Xiang Qian Lao [d,**]

[a] Division of Environment and Sustainability, the Hong Kong University of Science and Technology, Hong Kong, China
[b] Department of Civil and Environmental Engineering, the Hong Kong University of Science and Technology, Hong Kong, China
[c] Department of Mathematics, the Hong Kong University of Science and Technology, Hong Kong, China
[d] Jockey Club School of Public Health and Primary Care, the Chinese University of Hong Kong, Hong Kong, China

HIGHLIGHTS

- A mechanism-based parameterisation scheme was developed for transmission rate.
- Scale of population migration from Wuhan was incorporated.
- Population density had a non-linear (linearity index, 0.9) impact on disease spread.
- Transmission rate shows a negative and exponential temperature dependence.
- COVID-19 mitigation in densely populated and cold regions will be a great challenge.

GRAPHICAL ABSTRACT
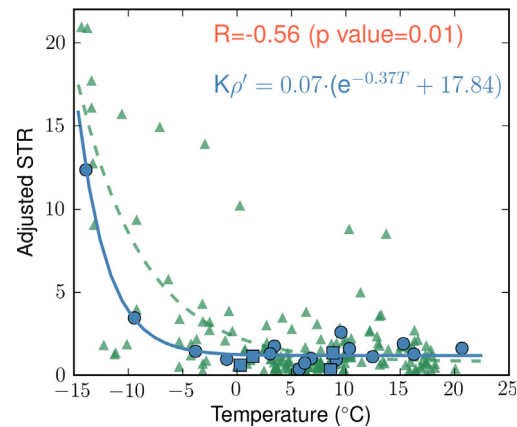
ARTICLE INFO

ABSTRACT

The novel coronavirus disease 2019 (COVID-19), which first emerged in Hubei province, China, has become a pandemic. However, data regarding the effects of meteorological factors on its transmission are limited and inconsistent. A mechanism-based parameterisation scheme was developed to investigate the association between the scaled transmission rate (STR) of COVID-19 and the meteorological parameters in 20 provinces/municipalities located on the plains in China. We obtained information on the scale of population migrated from Wuhan, the world epicentre of the COVID-19 outbreak, into the study provinces/municipalities using mobile-phone positioning system and big data techniques. The highest STRs were found in densely populated metropolitan areas and in cold provinces located in north-eastern China. Population density had a non-linear relationship with disease spread (linearity index, 0.9). Among various meteorological factors, only temperature was significantly associated with the STR after controlling for the effect of population density. A negative and exponential relationship was identified between the transmission rate and the temperature (correlation coefficient, −0.56; 99%

* Correspondence to: A.K.H. Lau, Academic Building R4332, the Hong Kong University of Science and Technology, Clear Water Bay, Kowloon, Hong Kong, China.
** Correspondence to: X.Q. Lao, Jockey Club School of Public Health and Primary Care, The Chinese University of Hong Kong, 421, 4/F School of Public Health, Prince of Wales Hospital, Sha Tin, N.T., Hong Kong, China.
E-mail addresses: alau@ust.hk (A.K.H. Lau), xqlao@cuhk.edu.hk (X.Q. Lao).

Imported scale
Population density

confidence level). The STR increased substantially as the temperature in north-eastern China decreased below 0 °C (the STR ranged from 3.5 to 12.3 when the temperature was between −9.41 °C and −13.87 °C), whilst the STR showed less temperature dependence in the study areas with temperate weather conditions (the STR was 1.21 ± 0.57 when the temperature was above 0 °C). Therefore, a higher population density was linearly whereas a lower temperature (<0 °C) was exponentially associated with an increased transmission rate of COVID-19. These findings suggest that the mitigation of COVID-19 spread in densely populated and/or cold regions will be a great challenge.

1. Introduction

As of 3 June 2020, the ongoing novel coronavirus disease 2019 (COVID-19) pandemic has caused >0.37 million deaths and 6.2 million confirmed cases of severe acute respiratory syndrome coronavirus 2 (SARS-CoV-2) infection around the world, and has aroused unprecedented public health concern (Dong et al., 2020; Giovanetti et al., 2020; Wu et al., 2020a; Zhu et al., 2020). Government-imposed interventions to decelerate the pandemic were applied throughout China, with a series of similar containment measures coordinated and implemented nationwide by central and local governments (Leung et al., 2020). These interventions comprised compulsory isolations and quarantines, social distancing policies, traffic and travel control, extension of the Chinese New Year vacation, closure of non-essential locations, an increase in SARS-CoV-2 testing capacity, and free treatment for severe cases of COVID-19 (Azman and Luquero, 2020). These nationwide government-imposed measures and mobility restrictions proved effective in suppressing the COVID-19 pandemic in China (Bogoch et al., 2020; Wu et al., 2020b).

Meteorological factors may affect the activity and viability of SARS-CoV-2 and thus influence its transmission efficiency (Casanova et al., 2010; van Doremalen et al., 2013). By analogy, it has been documented that a seasonal increase in temperature might have contributed to the decline in severe acute respiratory syndrome (SARS) infections in 2003 (Bi et al., 2007; Chan et al., 2011; Tan et al., 2005). In addition, the transmission of influenza viruses is often enhanced during cold weather (Xu et al., 2013). Therefore, it has been hypothesised that the transmission of COVID-19 may decrease as the temperature increases.

However, the evidence that meteorological factors may influence the transmission of COVID-19 is limited and equivocal. Some researchers have indeed reported a negative association between the temperature and the number of confirmed cases of COVID-19 in China, based on statistical models (Liu et al., 2020; Qi et al., 2020; Shi et al., 2020). By exploring the associations between the number of COVID-19 confirmed cases with meteorological factors in 30 provincial capital cities of China using non-linear regressions, Liu et al. (2020) concluded that each 1 °C increase in temperature was related to a decline in the daily counts of confirmed cases with a pooled relative risk of 0.80 (95% CI: 0.75, 0.85). Using a generalized additive model, Qi et al. (2020) found that each 1 °C increase in the temperature led to a decrease in the daily number of confirmed cases by 36% to 57% when relative humidity ranged from 67% to 85.5%. Similar negative associations were found in studies performed to examine COVID-19 outbreaks in other countries, such as Brazil, Turkey, and Spain (Prata et al., 2020; Şahin, 2020; Tobías and Molina, 2020). Using a generalized additive model, Prata et al. (2020) found that each 1 °C increase in temperature was associated with a decrease in the number of daily confirmed cases by −4.9% in the state capital cities of Brazil. Furthermore, it was revealed in an experimental laboratory study in Hong Kong that SARS-CoV-2 was highly stable in cold environments, but was sensitive to increased temperatures (Chin et al., 2020).

However, in China, Xie and Zhu (2020) applied a generalized additive model and found a positive linear relationship between the temperature and the number of confirmed cases of COVID-19 when the temperature was below 3 °C. A similar positive association was found

in analyses of data from Indonesia and New York (Bashir et al., 2020; Tosepu et al., 2020). By employing the spearman-rank correlation test on surveillance data of COVID-19 in Jakarta Indonesia, Tosepu et al. (2020) found a positive correlation coefficient of 0.39 between temperature and the COVID-19 pandemic. In another variation, Yao et al. (2020) explored data on the basic reproduction number of COVID-19 using multiple regression methods and found no association between the transmissibility of COVID-19 and temperature in 62 Chinese cities with >50 cases as of February 10, 2020. This conclusion was also reached by researchers who analysed data from Spain and Iran using various statistical models such as spatiotemporal modelling techniques, partial correlation coefficient and Sobol'-Jansen methods, and sensitivity and specificity analyses (Ahmadi et al., 2020; Briz-Redón and Serrano-Aroca, 2020; Jahangiri et al., 2020).

Furthermore, the association between the COVID-19 transmission rate and other meteorological factors is ambiguous. The findings of some studies show a negative association between the transmission rate and humidity (Liu et al., 2020; Qi et al., 2020; Şahin, 2020), whereas no significant dependence on humidity was reported in other studies (Ahmadi et al., 2020; Bashir et al., 2020; Tosepu et al., 2020; Yao et al., 2020).

Notably, due to its vast area, China has greater spatial variability in meteorological factors than the countries in which the above investigations were conducted (e.g., Iran, Turkey, Indonesia, and Spain). In addition, the scale of the population migration from Wuhan played a critical role in the transmission of COVID-19 in other provinces of China because it served as the seed of the COVID-19 spread. However, previous studies of the spread of COVID-19 in China have not considered the number of infected individuals who travelled from Wuhan to other provinces.

In China, the daily numbers of people traveling by airplane, train, and bus across the country can be tracked by using a combination of advanced mobile-phone positioning system and big data techniques. We thus developed a new mechanism-based parameterisation scheme to investigate the association between the transmission of COVID-19 and meteorological factors, with consideration of the scale of the population migration from Wuhan.

2. Data and methodology

2.1. Study region

We did not include Hong Kong, Taiwan, and Macau in this study because their health systems and government-imposed interventions differed greatly from those of mainland China. As altitude is closely related to various meteorological factors and may confound any relationship between meteorological factors and disease transmission, only data from provinces/municipalities on the plains of mainland China were examined. Thus, only provinces/municipalities with capital region at an elevation of <500 m were included, and those on plateaus or within mountainous regions were not investigated. The study region, as shown in Fig. S1 in the Supplementary Material, contained 16 provinces (Heilongjiang, Jilin, Liaoning, Hebei, Henan, Shandong, Shaanxi, Jiangsu, Zhejiang, Anhui, Hunan, Jiangxi, Fujian, Guangdong, Guangxi, and

Hainan) and four municipalities (Beijing, Tianjin, Shanghai, and Chongqing). All 20 administrative regions are denoted as 'provinces'.

2.2. Population density

Respiratory droplets and person-to-person contact are the major routes for the spread of SARS-CoV-2 (Lai et al., 2020). A high population density tends to increase the frequency of direct contact and thus accelerate this spread (Jahangiri et al., 2020; Şahin, 2020). The provincial average population densities of residential regions were estimated from their gross populations and area data, which were obtained from the China Statistical Yearbook 2019. Fig. S1 displays the spatial distribution of provincial average population densities across the study region. The greatest provincial averages of population densities existed in metropolitan regions, such as the Beijing-Tianjin (BT) region, the Yangtze River Delta (YRD) region (including Shanghai, Jiangsu, and Zhejiang), and the Pearl River Delta (PRD) region (including Guangdong).

2.3. Study period and meteorological factors

The study period was from 22 January to 29 February 2020. All of the study provinces had begun reporting confirmed cases of COVID-19 by 22 January 2020. By the end of February, the increase in the number of confirmed cases of COVID-19 had almost ceased, and there was no significant numbers of imported cases from overseas. Hourly meteorological data (comprising temperature, relative humidity, wind speed, cloud cover, precipitation, and air pressure) during the study period were obtained from the ground-based monitoring network of the World Meteorological Organization (WMO) global telecommunications system. Approximately 300 meteorological stations were located throughout the study provinces. The provincial averages of the meteorological parameters were estimated from observational data from all stations within each province. Time series of the provincial average of daily temperature for each province during the study period were shown in Fig. S2(a).

2.4. Imported scale index (ISI)

The cases of COVID-19 in the imported population from Wuhan served as the seed of the COVID-19 spread in each province outside Hubei. The percentage of the population that migrated from Wuhan into each studied province before the Chinese New Year (i.e., 25 January 2020) was denoted as the imported scale index (ISI) and was obtained from a big-data population-migration analysis tool developed by Baidu, Inc., an Internet company (https://qianxi.baidu.com/). The advanced mobile-phone positioning system and big-data framework of this tool enabled daily tracking of the population traveling by airplane, train, and bus from Wuhan to other locations across China. ISI data were obtained for the population migration from Wuhan to each studied province from 19 to 23 January 2020, a period between the first official announcement of COVID-19 and the lockdown of Wuhan.

2.5. Cumulative confirmed cases of COVID-19

The cumulative numbers of confirmed cases of COVID-19 for each studied province during the study period were obtained from a data repository at Johns Hopkins University Center for Systems Science and Engineering (CSSE). The CSSE has been collating COVID-19 data from various official sources around the world for cleaning and normalising (Dong et al., 2020). The CSSE database has been extensively used in a range of COVID-19 research projects (Kuster et al., 2020). Time series of cumulative number of confirmed cases for each province during the study period were shown in Fig. S2(b).

2.6. Parameterisation scheme

The transmissibility of COVID-19 can be indicated by factors such as basic reproduction number (the number of new infections each case generates) (Yao et al., 2020) and doubling time (the amount of time when the number of cases doubles) (Nunes-Vaz, 2020). Based on this physical understanding, the transmission rate of COVID-19 for a given region is defined as the number of new infections each case generates per unit of time. Thus, the cumulative number of confirmed cases (N) of COVID-19 on date t can be expressed as:

$$N = N_0 \cdot K \cdot (t - t_0) \tag{1}$$

where N_0 represents the number of cases of COVID-19 imported from Wuhan on initial date t_0, and K represents the average transmission rate of COVID-19 during the study period. The use of the cumulative number of confirmed cases to derive the average transmission rate has several strengths. First, compared to the noisy daily data, the cumulative number of confirmed cases is more stable. Meanwhile, the daily reported cases are a small fraction of true cases. The use of the cumulative number of confirmed cases decreases the deviation in the calculation of transmission rate. In addition, there can be an incubation period and a delay to the confirmation of cases resulting from limited detection and testing capacity. This greatly affects the accuracy of the daily data. The use of the cumulative number of confirmed cases minimises the confounding effects of the time delay.

The number of cases of COVID-19 imported from Wuhan on initial date t_0 can be expressed as follows:

$$N_0 = U \cdot I \cdot \gamma_0 \tag{2}$$

where U represents the total population that migrated from Wuhan on date t_0; I is the ISI, representing the percentage of the population imported into each province on date t_0; and γ_0 is the initial COVID-19 rate in this population.

Then, the transmission rate can be estimated by:

$$K = \frac{N}{N_0 \cdot (t - t_0)} = \frac{N}{U \cdot I \cdot \gamma_0 \cdot (t - t_0)} = k_0 \cdot \frac{N}{I} \tag{3}$$

where $k_0 = \frac{1}{U \cdot \gamma_0 \cdot (t - t_0)}$ is a constant, representing the integrated effect of the total population migrating from Wuhan to other provinces on the initial date, the initial infection rate, and the time period. The transmission rate is affected by multiple factors such as population density, meteorological factors, and other factors (e.g., containment measures). Therefore, it can be expressed as:

$$K = P \cdot M \cdot \varepsilon \tag{4}$$

where P represents the effect of population density; M represents the effect of various meteorological factors, such as temperature, relative humidity, wind speed, cloud cover, precipitation, and pressure; and ε represents the effect of other factors.

Because population density may have a linear or non-linear effect on the transmission rate, its effect can be expressed as follows:

$$P = \beta \cdot \rho^{\alpha} \tag{5}$$

where ρ is the average population density for the study region; α is a linearity index; and β is a constant, scaling the magnitude of this effect.

Then, the transmission rate (K) can be expressed as:

$$K = \beta \cdot \rho^{\alpha} \cdot M \cdot \varepsilon \tag{6}$$

To facilitate data comparison among the provinces, the transmission rate was scaled by removing the effect of k_0, yielding a scaled transmission rate (STR; K') that can be estimated by:

$$K' = \frac{K}{k_0} = \frac{N}{I} \qquad (7)$$

The STR is affected by population density, meteorological factors, and other factors, and thus can also be expressed as follows:

$$K' = \frac{\beta \cdot \rho^\alpha \cdot M \cdot \varepsilon}{k_0} = k \cdot \rho^\alpha \cdot M \qquad (8)$$

where $k = U \cdot \gamma_0 \cdot (t - t_0) \cdot \beta \cdot \varepsilon$ is an integrated coefficient that denotes the effects of the total population migrating from Wuhan to other provinces on the initial date, the initial infection rate, the time period, and remaining factors.

3. Results

3.1. Meteorological values

The spatial distributions of the provincial averages of temperature, relative humidity, wind speed, cloud cover, precipitation, and pressure in the study region from 22 January to 29 February 2020 were analysed. Results are presented in Fig. S3 in the Supplementary Material. In general, a north-to-south increasing gradient was found for temperature, relative humidity, cloud cover, and precipitation. The average temperatures in north-eastern China (e.g., Heilongjiang, Jilin, and Liaoning) were below 0 °C. The relative humidity and precipitation on the north China plain (e.g., Hebei and Shaanxi) were lower than those in north-eastern China. The highest relative humidity, cloud cover, and precipitation occurred in provinces within central China (e.g., Chongqing and Hunan). The wind speeds in provinces near the coast (e.g., Shandong, Zhejiang, and Hainan) were generally much higher than those in inland provinces. As the study region was on a plain, there was relatively uniform elevation and therefore less spatial variability of air pressure.

3.2. Scaled transmission rate (STR)

The scaled transmission rate (STR) for each province can be estimated based on the imported scale index (ISI, I) at the beginning of the study period (i.e., from 19 to 23 January 2020) and the cumulative number of confirmed cases (N) at the end of the study period (i.e., 29 February 2020). Panel (a) of Fig. 1 shows the spatial distribution of the ISI (I) for each study province. It can be seen that a higher portion of Wuhan's population migrated to provinces in central and southern China (e.g., Henan, Hunan, Anhui, Jiangxi, and Guangdong), with the highest ISI (5.8%) in Henan. Panel (b) of Fig. 1 shows the spatial

distribution of the cumulative number of confirmed cases of COVID-19 for each province (N) on 29 February 2020. The number of confirmed cases ranged from 93 in Jilin to 1349 in Guangdong. More confirmed cases were detected in the study provinces in central or southern China, which share a pattern similar to the ISI at the beginning of the study period.

Based on the ISI (I) and the cumulative number of confirmed cases (N), the STR ($K' = N/I$) during the study period was estimated for each province. The results are shown in panel (a) of Fig. 2. The highest transmission rates were found in the densely populated metropolitan areas (e.g., the BT, YRD, and PRD regions) and in the provinces in north-eastern China that experienced the lowest temperatures (e.g., Heilongjiang and Jilin).

3.3. Adjusted STR

The effect of population density on the COVID-19 spread may be linear or non-linear. The spatial correlation between the STR and population density was assessed with different α values. As shown in Fig. S4, increasing the α value from 0.1 to 2.0 with an interval of 0.1 resulted in positive correlation coefficients for all α values, which confirmed that a higher population density tended to increase the risk of COVID-19 spread. In addition, the maximum correlation coefficient occurred with an α value of 0.9, which indicates that the population density had an approximately linear relationship with the transmission rate.

Therefore, the α value was assumed to be one in this study. The STR can then be adjusted by controlling for the effect of population density, resulting in the adjusted STR as follows:

$$K_\rho' = \frac{K'}{\rho} = k \cdot M \qquad (9)$$

Panel (b) of Fig. 2 shows the spatial distribution of the adjusted STR for each province. After controlling for the effect of population density, the adjusted STR in the metropolitan areas (e.g., the BT, YRD, and PRD regions) decreased to a level similar to that of most other provinces. However, the highest adjusted STR was still found in the study provinces in north-eastern China, such as Heilongjiang and Jilin. These results indicated that the high transmission rates in the metropolitan areas were largely determined by their high population densities, whereas the high transmission rates in the less-populated provinces in north-eastern China were determined by other factors.
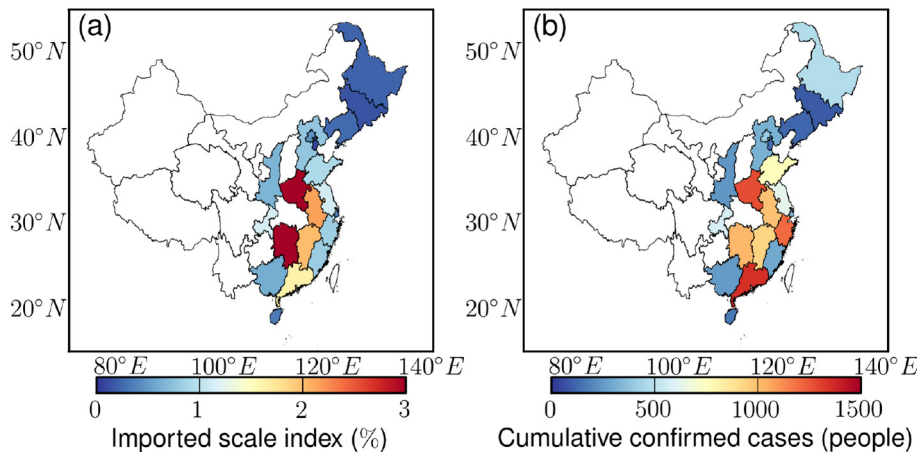

Fig. 1. (a) Spatial distribution of the imported scale index (ISI, I) for each province located on plains in China from 19 to 23 January 2020. (b) Spatial distribution of the cumulative number of confirmed cases (N) of COVID-19 for each province located on plains in China on 29 February 2020.
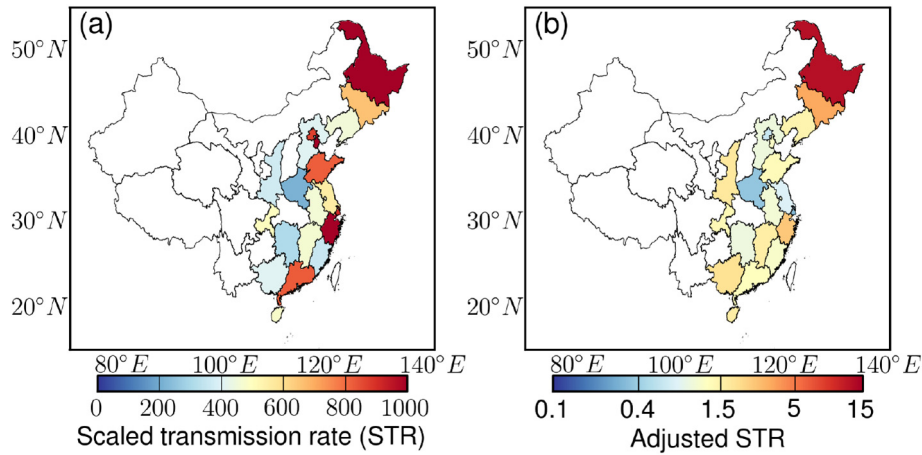
Fig. 2. Spatial distribution of (a) the scaled transmission rate (STR, $K' = N/I$) and (b) the adjusted STR ($K_\rho' = K'/\rho$, further controlling for population density) for each province located on plains in China.

3.4. Association between adjusted STR and meteorology

The spatial associations between the adjusted STR and various meteorological factors were further investigated. Fig. 3 shows the spatial association between the adjusted STR and temperature for the study provinces/municipalities (blue dots and squares), whilst the associations between the adjusted STR and other meteorological variables are presented in Fig. S5. Among these meteorological factors, only temperature showed a significant association with the adjusted STR (correlation coefficient, −0.56; 99% confidence level, mathematical calculation of the correlation coefficient and confident level were shown in Section S1 in Supplementary Material).

In addition, a negative exponential relationship was identified between the adjusted STR and temperature, which is expressed as follows:

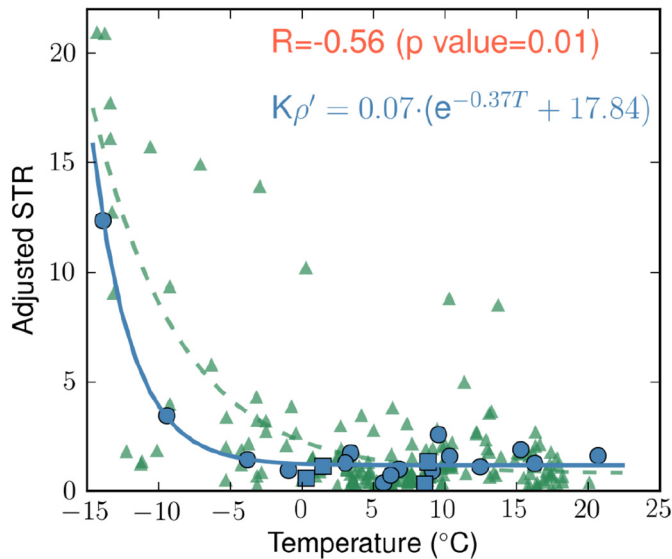$$K_\rho' = 0.07 \cdot \left(e^{-0.37 \cdot T} + 17.84\right) \tag{10}$$

Fig. 3. Spatial association between the adjusted STR (K_ρ') and temperature for provinces located on plains in China. The blue curve shows the association between the adjusted STR and temperature for the 16 studied provinces (blue dots) and the four municipalities (blue squares) in China. The green curve shows the association between the adjusted STR and temperature for all 191 cities with a population larger than one million in the 16 provinces.

The adjusted STR substantially increased as the temperature decreased below 0 °C in north-eastern China. The average of the adjusted STR was estimated to be 1.21 ± 0.57 for provinces with temperatures above 0 °C, whilst the adjusted STR range was much higher from 3.5 to 12.3 when the temperature range was −9.41 °C to −13.87 °C (mathematical calculation of the mean value was shown in Section S1 in Supplementary Material). Under temperate weather conditions, the adjusted STR showed less temperature dependence. These results suggest that it will be very challenging to mitigate the spread of COVID-19 in high-latitude regions that experience more cold weather.

To test the robustness of the association, we conducted a sensitivity analysis using all 191 cities with a population above one million in the 16 provinces, and a similar association was observed (the green curve in Fig. 3).

4. Discussion

To the best of our knowledge, this is the first investigation of the association between meteorological factors and COVID-19 transmission that considers effect of the scale of population migration from Wuhan, the epicentre of COVID-19, into the study provinces in China. We found greater migration from Wuhan at the beginning of the study period (i.e., from 19 to 23 January 2020) to each province was associated with a greater number of cumulative confirmed cases of COVID-19 at the end of the study period (i.e., 29 February 2020) in the province. In addition, we found that a higher population density was associated with an increased risk of COVID-19 spread and that the population density had a non-linear relationship (linearity index of 0.9) with the transmission rate. Finally, we determined that temperature showed a negative and exponential association with the transmission rate of COVID-19 after controlling for population density, the number of COVID-19 cases in those who had migrated from Wuhan on the initial date, the time period, and other factors. The adjusted STR ranged from 3.5 to 12.3 when the temperature was between −9.41 °C and −13.87 °C, and it was 1.21 ± 0.57 when the temperature was above 0 °C. No significant associations were observed between the adjusted STR and the other meteorological factors.

We performed a series of data standardization before using the method. First, we excluded data on plateaus or within mountainous regions in China. Only provinces/municipalities with capital region at an elevation of <500 m were used. Second, we excluded Hong Kong, Taiwan, and Macau in this study because their health systems and government-imposed interventions differed greatly from those of mainland China. Third, we excluded Hubei province in our data analysis because the health system of Hubei province was overwhelmed and

therefore the data on the number of cases and the transmission pattern of COVID-19 in Hubei might not be as reliable as data from other provinces. Fourth, the cumulative numbers of confirmed cases of COVID-19 were cleaned and normalized by the CSSE (e.g., tidying dates and consolidating several files into normalized time series).

This study has several important strengths. First, we investigated the association of temperature with the transmission of COVID-19 based on the imported scale of infected cases from Wuhan, the epicentre of COVID-19. Second, China has great spatial variance in meteorological factors, which enabled us to detect the effects of temperature on the transmission of COVID-19. As shown in Fig. S2 in the Supplementary Material, the provincial average temperature during the study period ranged from −13.8 °C to 20.7 °C. Therefore, the climates in China were diverse, covering both cold and warm weathers. The results from China provide a clue for us to understand the transmission of COVID-19 in other countries with different climates. Third, similar government-imposed interventions to decelerate the pandemic were applied across the study provinces, which helped to minimise the potential confounding effects of policy interventions. Lastly, the COVID-19 almost simultaneously spread in different provinces over China, facilitating the intercomparison among the provinces. These unique characteristics make China an ideal region for the research on the association between meteorological factors and the transmissibility of COVID-19.

The findings of our study show that both the ISI and population density played key roles in COVID-19 spread in the study provinces. More confirmed cases of COVID-19 were reported in the provinces with high ISI in central and southern China (Fig. 1). However, after controlling for ISI, high transmission rates were observed not only in the densely populated metropolitan regions but also in high-latitude regions with relatively low population densities (Fig. 2a). After further controlling for population density, the high transmission rates disappeared in the densely populated metropolitan regions but remained in the high-latitude regions (Fig. 2b), indicating that factors other than ISI and population density must drive high transmission rates in the high-latitude regions. Our association analyses further show that the low temperature in the high-latitude regions may have been the driving force for COVID-19 spread (Fig. 3).

The outbreak of the SARS-CoV in 2003 declined in summer, suggesting that respiratory viruses spread more effectively in cold environment. However, the evidence that temperature may influence the transmission rate of COVID-19 is limited and equivocal. The results on the temperature-dependent spread of COVID-19 in the present study are similar to the effects of temperature on the spread of other respiratory-borne infectious diseases such as SARS and influenza (Tan et al., 2005). Our results provided a new evidence that a lower temperature (<0 °C) was associated with an increased transmission rate of COVID-19.

Meanwhile, the results are in line with those of other epidemiological and laboratory studies, in which it was determined that the transmission rate of COVID-19 had a negative correlation with temperature (Chin et al., 2020; Liu et al., 2020; Qi et al., 2020). The underlying hypothesis is that the increase in temperature reduces the activity and viability of SARS-CoV-2 and thus influences its transmission efficiency. According to the laboratory results, the resistance the SARS-CoV-2 was 5 min at 70 °C, but the virus was highly stable at 4 °C, indicating that temperature decrease may increase viability of SARS-COV-2 and its stability on surfaces (Chin et al., 2020).

Data on the impact of temperature is limited and inconsistent. Previous studies in China did not consider the effect of imported scale of infected individuals from Wuhan into other provinces of China. However, the imported cases from Wuhan served as the seed for COVID-19 spread outside Hubei provinces and thus played an important role in disease transmission. As shown in Fig. 1, more confirmed cases of COVID-19 were detected in the study provinces located in central or southern China. The temperature values in these provinces were much higher than those in northern China. As a result, a positive correlation coefficient can be found between the temperature and the

number of confirmed cases among the provinces. However, after considering the impact of the imported scale from Wuhan, a negative correlation coefficient was found between temperature and transmission rate. This is possibly one of the reasons of inconsistent results of previous studies in China.

No significant dependence on humidity was found, however, which is also consistent with the findings of several other studies in China, Iran, New York, and Indonesia (Ahmadi et al., 2020; Bashir et al., 2020; Tosepu et al., 2020; Yao et al., 2020). As shown in Fig. S3, provincial average of relative humidity ranged from 59% to 83% during the study period. With more datasets become available over a longer period of time, more analyses are warranted to further investigate the impacts of humidity. In addition, analysing data in other countries, with an expanding coverage of relative humidity, is critical to improve our understanding of the impact of relative humidity.

The negative and exponential relationship observed in cold weather conditions suggests that cold regions (e.g., high-latitude regions) are at increased risk for the spread of COVID-19. Under temperate weather conditions, the transmission rate showed less temperature dependence. However, many factors are related to the spread of COVID-19, such as intervention policies, vulnerable population, ventilation, and personal hygiene. Therefore, our results should not be interpreted as meaning that the arrival of summer in the northern hemisphere will effectively dissipate the COVID-19 pandemic in warm regions. These results are consistent with the fact that warm countries, such as Iran and Australia, are experiencing a rapid spread of COVID-19.

This study has a couple of limitations. First, although the parameterisation scheme used in this study explicitly accounted for the effects of some essential factors, such as the imported scale of infected individuals, the population density, and meteorological factors, the effects of remaining factors (e.g., elevation, intervention strategies, socioeconomic status, and medical resources) were combined into the ε value. For example, to minimise the confounding effect from the elevation, only data from provinces/municipalities on the plains of mainland China were examined. The provinces on plateaus or within mountainous regions (marked as blank areas in the geographical plots) were not investigated in the present study. The underlying reason is that we aim to keep a balance between the sufficient types of climates and minimising all possible confounding effects (including elevation) in the analyses. Further studies are warranted, using a more complicated model to explicitly address the effects of these potential confounders, such as elevation and intervention strategies. Second, the study period was short, so further research over a longer duration is required to investigate seasonal variations in the transmission rate of COVID-19.

This study focused on the development of the mechanism-based parameterisation scheme to investigate the association between the transmission rate of COVID-19 and meteorological parameters. The performance of the proposed mechanism in the present research work need further evaluation by appropriately applying it in other countries with an increase in the temperature and with the reach of the warm climates. Further studies are warranted to apply our parameterisation scheme in other regions to enhance our understanding of the meteorological impacts on the transmission of COVID-19. With more regions incorporated, the confounding effects of the government-imposed interventions will be explicitly taken into account. In addition, with more dataset become available in the near future, comprehensive analyses will be conducted to investigate the impacts of meteorological factors during the seasonal transition (i.e., arrival of summer in the northern hemisphere and of winter in the southern hemisphere). Furthermore, complicated statistical models can be applied to reveal their associations. The Modal Assurance Criterion is a statistical indicator showing a degree of consistency between two mode shapes (Pastor et al., 2012). It is often used to pair modes shapes derived from analytical models with those obtained experimentally. Future studies can use it to reveal the association between transmission rate and meteorological factors when more data become available.

This study analysed spatial correlation between the transmission rate of COVID-19 and meteorological factors for 20 provinces located on plains in China (shown in Fig. 3). A few challenges exist in the assessment of the temporal association between the transmission rate of COVID-19 and meteorological parameters. First, during a short period (e.g., one month), the temporal variations in the meteorological factors may not be significant. Second, government interventions could be implemented during the study period. These interventions affect the spread of COVID-19, and thus confound the assessment of the impacts of meteorological factors. Future studies can assess the temporal association between the transmission rate and meteorological factors by taking into account the effects of the potential confounders.

5. Conclusions

A higher population density was associated with an increased risk of COVID-19 spread, and the population density had a non-linear (linearity index of 0.9) relationship with disease spread. Among various meteorological factors, only temperature was associated with the transmission rate of COVID-19 after controlling for the effect of population density. A negative and exponential relationship was observed between the transmission rate of COVID-19 and temperature (correlation coefficient, −0.56; 99% confidence level). The transmission rate substantially increased as the temperature decreased below 0 °C in north-eastern China (the STR ranged from 3.5 to 12.3 when the temperature was between −9.41 °C and −13.87 °C), whilst it showed less temperature dependence under temperate weather conditions (the STR was 1.21 ± 0.57 when the temperature was above 0 °C). These results suggest that it will be a great challenge to mitigate COVID-19 spread in densely populated and/or cold regions.

Contributors

AKHL supervised the study. JCHF, CQL, JWMC, and YCB obtained the data. CQL, YMZ, MSH, and YQZ searched the literature. CQL, CG, and DWY analysed the data. CQL and XQL drafted the manuscript. AKHL and XQL obtained the funding. All authors critically revised the manuscript.

Declaration of competing interest

The authors declare that they have no known competing financial interests or personal relationships that could have appeared to influence the work reported in this paper.

Acknowledgments

Appendix A. Supplementary data

Supplementary data to this article can be found online at https://doi.org/10.1016/j.scitotenv.2020.140348.

References

Ahmadi, M., Sharifi, A., Dorosti, S., Ghoushchi, S.J., Ghanbari, N., 2020. Investigation of effective climatology parameters on COVID-19 outbreak in Iran. Sci. Total Environ. 729, 138705 (1-7).

Azman, A.S., Luquero, F.J., 2020. From China: hope and lessons for COVID-19 control. Lancet Infect. Dis. 0.

Bashir, M.F., Ma, B., Bilal, Komal, B., Bashir, M.A., Tan, D., Bashir, M., 2020. Correlation between climate indicators and COVID-19 pandemic in New York, USA. Sci. Total Environ. 728, 138835.

Bi, P., Wang, J., Hiller, J.E., 2007. Weather: driving force behind the transmission of severe acute respiratory syndrome in China? Intern. Med. J. 37, 550–554.

Bogoch, I.I., Watts, A., Thomas-Bachli, A., Huber, C., Kraemer, M.U.G., Khan, K., 2020. Pneumonia of unknown aetiology in Wuhan, China: potential for international spread via commercial air travel. J. Travel Med. 27.

Briz-Redón, Á., Serrano-Aroca, Á., 2020. A spatio-temporal analysis for exploring the effect of temperature on COVID-19 early evolution in Spain. Sci. Total Environ. 728, 138811 (1-7).

Casanova, L.M., Jeon, S., Rutala, W.A., Weber, D.J., Sobsey, M.D., 2010. Effects of air temperature and relative humidity on coronavirus survival on surfaces. Appl. Environ. Microbiol. 76, 2712–2717.

Chan, K.H., Peiris, J.S.M., Lam, S.Y., Poon, L.L.M., Yuen, K.Y., Seto, W.H., 2011. The Effects of Temperature and Relative Humidity on the Viability of the SARS Coronavirus (Hindawi).

Chin, A.W.H., Chu, J.T.S., Perera, M.R.A., Hui, K.P.Y., Yen, H.-L., Chan, M.C.W., Peiris, M., Poon, L.L.M., 2020. Stability of SARS-CoV-2 in different environmental conditions. Lancet Microbe 0.

Dong, E., Du, H., Gardner, L., 2020. An interactive web-based dashboard to track COVID-19 in real time. Lancet Infect. Dis. 533–534.

van Doremalen, N., Bushmaker, T., Munster, V.J., 2013. Stability of Middle East respiratory syndrome coronavirus (MERS-CoV) under different environmental conditions. Euro Surveill. Bull. Eur. Sur Mal. Transm. Eur. Commun. Dis. Bull. 18.

Giovanetti, M., Benvenuto, D., Angeletti, S., Ciccozzi, M., 2020. The first two cases of 2019-nCoV in Italy: where they come from? J. Med. Virol. 92, 518–521.

Jahangiri, M., Jahangiri, M., Najafgholipour, M., 2020. The sensitivity and specificity analyses of ambient temperature and population size on the transmission rate of the novel coronavirus (COVID-19) in different provinces of Iran. Sci. Total Environ. 728, 138872.

Kuster, G.M., Pfister, O., Burkard, T., Zhou, Q., Twerenbold, R., Haaf, P., Widmer, A.F., Osswald, S., 2020. SARS-CoV2: should inhibitors of the renin–angiotensin system be withdrawn in patients with COVID-19? Eur. Heart J. 1–3.

Lai, C.-C., Shih, T.-P., Ko, W.-C., Tang, H.-J., Hsueh, P.-R., 2020. Severe acute respiratory syndrome coronavirus 2 (SARS-CoV-2) and coronavirus disease-2019 (COVID-19): the epidemic and the challenges. Int. J. Antimicrob. Agents 55, 105924.

Leung, K., Wu, J.T., Liu, D., Leung, G.M., 2020. First-wave COVID-19 transmissibility and severity in China outside Hubei after control measures, and second-wave scenario planning: a modelling impact assessment. Lancet 395, 1382–1393.

Liu, J., Zhou, J., Yao, J., Zhang, X., Li, L., Xu, X., He, X., Wang, B., Fu, S., Niu, T., et al., 2020. Impact of meteorological factors on the COVID-19 transmission: a multi-city study in China. Sci. Total Environ. 726, 138513.

Nunes-Vaz, R., 2020. Visualising the doubling time of COVID-19 allows comparison of the success of containment measures. Global Biosecurity 1 (3). https://doi.org/10.31646/gbio.61 p.None.

Pastor, M., Binda, M., Harčarik, T., 2012. Modal Assurance Criterion. Procedia Eng 48, 543–548.

Prata, D.N., Rodrigues, W., Bermejo, P.H., 2020. Temperature significantly changes COVID-19 transmission in (sub)tropical cities of Brazil. Sci. Total Environ. 729, 138862 (1-7).

Qi, H., Xiao, S., Shi, R., Ward, M.P., Chen, Y., Tu, W., Su, Q., Wang, W., Wang, X., Zhang, Z., 2020. COVID-19 transmission in mainland China is associated with temperature and humidity: a time-series analysis. Sci. Total Environ. 728, 138778 (1-6).

Şahin, M., 2020. Impact of weather on COVID-19 pandemic in Turkey. Sci. Total Environ. 728, 138810.

Shi, P., Dong, Y., Yan, H., Zhao, C., Li, X., Liu, W., He, M., Tang, S., Xi, S., 2020. Impact of temperature on the dynamics of the COVID-19 outbreak in China. Sci. Total Environ. 728, 138890.

Tan, J., Mu, L., Huang, J., Yu, S., Chen, B., Yin, J., 2005. An initial investigation of the association between the SARS outbreak and weather: with the view of the environmental temperature and its variation. J. Epidemiol. Community Health 59, 186–192.

Tobías, A., Molina, T., 2020. Is temperature reducing the transmission of COVID-19? Environ. Res. 186, 109553 (1-2).

Tosepu, R., Gunawan, J., Effendy, D.S., Ahmad, L.O.A.I., Lestari, H., Bahar, H., Asfian, P., 2020. Correlation between weather and Covid-19 pandemic in Jakarta, Indonesia. Sci. Total Environ. 725, 138436.

Wu, F., Zhao, S., Yu, B., Chen, Y.-M., Wang, W., Song, Z.-G., Hu, Y., Tao, Z.-W., Tian, J.-H., Pei, Y.-Y., et al., 2020a. A new coronavirus associated with human respiratory disease in China. Nature 579, 265–269.

Wu, J.T., Leung, K., Leung, G.M., 2020b. Nowcasting and forecasting the potential domestic and international spread of the 2019-nCoV outbreak originating in Wuhan, China: a modelling study. Lancet 395, 689–697.

Xie, J., Zhu, Y., 2020. Association between ambient temperature and COVID-19 infection in 122 cities from China. Sci. Total Environ. 724, 138201.

Xu, Z., Hu, W., Williams, G., Clements, A.C.A., Kan, H., Tong, S., 2013. Air pollution, temperature and pediatric influenza in Brisbane, Australia. Environ. Int. 59, 384–388.

Yao, Y., Pan, J., Liu, Z., Meng, X., Wang, W., Kan, H., Wang, W., 2020. No association of COVID-19 transmission with temperature or UV radiation in Chinese cities. Eur. Respir. J. https://doi.org/10.1183/13993003.00517-2020 (Published online April 8, 2020).

Zhu, N., Zhang, D., Wang, W., Li, X., Yang, B., Song, J., Zhao, X., Huang, B., Shi, W., Lu, R., et al., 2020. A novel coronavirus from patients with pneumonia in China, 2019. N. Engl. J. Med. 382, 727–733.